



**Manchester
Metropolitan
University**

Betlem, K, Hoksbergen, S, Mansouri, N, Down, M, Losada-Perez, P, Eersels, K, van Grinsven, B, Cleij, T, Kelly, P, Sawtell, D, Zubko, M, Banks, C and Peeters, M (2018) Real-time analysis of microbial growth by means of the Heat-Transfer Method (HTM) using *Saccharomyces cerevisiae* as model organism. *Physics in Medicine*, 6. pp. 1-8. ISSN 2352-4510

Downloaded from: <https://e-space.mmu.ac.uk/620887/>

Publisher: Elsevier

DOI: <https://doi.org/10.1016/j.phmed.2018.05.001>

Usage rights: Creative Commons: Attribution-Noncommercial-No Derivative Works 4.0

Please cite the published version

<https://e-space.mmu.ac.uk>



Real-time analysis of microbial growth by means of the Heat-Transfer Method (HTM) using *Saccharomyces cerevisiae* as model organism



K. Betlem^a, S. Hoksbergen^a, N. Mansouri^a, M. Down^a, P. Losada-Pérez^b, K. Eersels^c,
B. van Grinsven^c, T.J. Cleij^c, P. Kelly^a, D. Sawtell^a, M. Zubko^a, C. Banks^a, M. Peeters^{a,*}

^a Manchester Metropolitan University, Advanced Materials and Surface Engineering Research Centre, Div. of Chemistry & Environmental Science, John Dalton Building, Chester Street, M15GD, Manchester, United Kingdom

^b Soft Matter Physics Laboratory, Université Libre de Bruxelles (ULB), Campus La Plaine, CP223, Boulevard du Triomphe, 1050, Brussels, Belgium

^c Maastricht Science Programme, Maastricht University, P.O. Box 616, 6200 MD, Maastricht, The Netherlands

ARTICLE INFO

Keywords:

Biosensors
Thermal detection
Heat-transfer method
Microorganism growth
S. cerevisiae
3D-printing

ABSTRACT

In this manuscript, we explore the use of the Heat-Transfer Method (HTM) for the *real-time* analysis of microbial growth using *Saccharomyces cerevisiae* as a model organism. The thermal responses of gold electrodes upon exposure to suspensions of *S. cerevisiae* (wild type strain DLY640) concentrations were monitored, demonstrating an increase in thermal resistance at the solid-liquid interface with higher concentrations of the microorganism. Flow cells were manufactured using 3D-printing to facilitate longitudinal experiments.

We can clearly discriminate between the growth of *S. cerevisiae* under optimal conditions and under the influence of factors that inhibit the replication process, such as the use of nutrient depleted growth medium, elevated temperature, and the presence of toxic compounds. In addition, it is possible to determine the kinetics of the growth process and quantify yeast replication which was demonstrated by measuring a mutant temperature sensitive strain.

This is the first time HTM has been used for the *real-time* determination of factors that impact microbial growth. Thermal sensing is low-cost, offers straightforward analysis and measurements can be performed on-site. Due to the versatility of this method, this platform can be extended to monitor other microorganisms and in particular to study the response of bacteria to selected antibiotics.

1. Introduction

Over recent years, there has been a growing demand to develop label-free, low-cost, sensitive, and easy to operate biosensor platforms [1,2]. The Heat-Transfer Method (HTM) is a promising emerging technology, whose measurement concept is based on the analysis of thermal transport through functional interfaces [3]. It is a versatile strategy that can correlate changes in the thermal resistance at the solid-liquid interface to a range of effects including DNA denaturation [4], target-receptor binding [5,6] and phase transitions in lipid vesicles [7]. The aim of this work was to evaluate the growth of microorganisms using HTM, an application that has not yet been explored.

Yeast was used as a model organism, since it is easy to manipulate, low-cost, does not require handling in specialized lab facilities and it bears a high similarity to higher eukaryotic cells [8,9]. We will focus on *Saccharomyces cerevisiae*, the microorganism behind the most common type of fermentation that reproduces by a division process known as budding [10,11]. Providing sufficient nutrients are present, *S. cerevisiae*

doubles in number every 100–120 min [12]. Contrary to bacteria, *S. cerevisiae* lacks self-mobility in solutions and therefore it is expected that the yeast will sink to the electrodes and replicate there, which will have a significant impact on the thermal resistance at the interface [13]. In this work, we have used laboratory strains DLY640 as a standard wild type strain (WT) and DLY1108 a mutant strain (*cdc13-1* mutation), with both strains originating from the Rothstein lab [14]. The mutant strain has an optimum growth temperature between 22 and 24 °C, and forms DNA defects when grown above 30 °C [15,16], while the WT strain has an optimum growth temperature of approximately 35 °C [17]. We have considered the use of various electrodes and evaluated the capability of the yeast cells to adhere to these surfaces, which is required to measure changes at the solid-liquid interface with increasing yeast concentrations.

However, the drawback of working with this microorganism was that carbon dioxide is produced in the budding process [18,19]. The gas builds up with the current design of the flow cell and will interfere significantly with the thermal analysis, since carbon dioxide has a

* Corresponding author.

E-mail address: m.peeters@mmu.ac.uk (M. Peeters).

distinctly higher thermal resistance than buffered solutions that are currently used in HTM [20]. Attempts were made to remove the build-up of gas with a peristaltic pump connected to the HTM set up, but this either interfered significantly with the thermal signal or removed the budding yeast cells from the surface. Therefore, the flow cells were redesigned to enable gas removal and manufactured using 3D-printing techniques [21].

Subsequently, the effect on yeast growth kinetics was studied by varying the growth temperature and by inhibiting yeast growth via either a nutrient deficient medium, the addition of copper or by thermal elimination. A mutated strain was employed that is known to exhibit different optimal growth temperatures than the WT [22], which is reflected in the thermal signal.

Clear inhibition of yeast growth was observed when insufficient nutrients are present or when the yeast cells are exposed to high temperatures. Surfaces made of copper, or the addition of copper ions, have strong antimicrobial properties against a variety of microorganisms [23]. While there are on-going debates on the exact mode of action for antimicrobial efficacy, several reports suggest that copper surfaces inactivate *S. cerevisiae* within minutes in a process called contact-mediated killing [24,25]. Results obtained with HTM indicate that the copper ions added to yeast cultures inhibit growth or, if present in sufficiently high concentration, kill the yeast cells. These results were confirmed using standard plating techniques [26] or by determining concentrations of yeast cells spectrophotometrically [27]. While plating techniques are low-cost, they are not able to quantify yeast growth or determine kinetics. Disadvantages of UV-vis include that this method does not discriminate between alive and dead cells and *real-time* analysis is not possible.

In this paper, we present the first use of HTM to study microorganism growth using yeast as model organism. Compared to conventional techniques, HTM has significant advantages in its simplicity, low-cost and providing sensitive data that can be monitored in *real-time*. Because of the versatility of this thermal technique, this is a very promising method that can be extended to evaluate growth of other microorganisms such as bacteria and fungi. In particular, we envisage this work as a reference method to monitor the response of different microorganisms to various drugs.

2. Materials and methods

2.1. Chemicals and equipment

Yeast Extract, Peptone Bacteriological, Agar Bacteriological (Agar NO.1), D (+)-Glucose, Glycerol and copper (II) sulfate were all obtained from Fisher Scientific (Basingstoke, UK). Adenine sulfate was purchased from Alfa Aesar (Heysham, United Kingdom). Gold-coated electrodes were made from a doped silicon chips of $1 \times 1 \text{ cm}^2$ size and 450 μm thickness in (100) crystalline orientation. The substrates were prepared by physical vapor deposition at $5 \times 10^{-5} \text{ Pa}$. First, an adhesive chromium layer of 20 nm was deposited onto the silicon substrates, on top of which a 100 nm gold layer was evaporated as described in ref 20. A thin layer of Au/Pd was applied on a Si substrate (Sigma, United Kingdom) using a SC7640 sputter device from Polaron (Hertfordshire, United Kingdom).

Yeast extract peptone dextrose [YPED] (containing 1% yeast extract, 2% peptone bacteriological, 2% D (+)-glucose and 0.03% adenine sulfate) was used as a standard growth broth. Solid YEPD plates contained additionally 2% agar. Ex-YEPD was an exhausted medium obtained after incubating WT yeast cells in fresh YEPD broth for at least 72 h at 30 °C. After incubation the culture was centrifuged, and the supernatant was autoclaved to obtain sterile and nutrient-deficient ex-YEPD.

2.2. Cryo-storage of yeast cells

A fresh colony of yeasts taken from YEPD agar plate, suspended and grown in 250 mL of YEPD broth at $23 \pm 0.05 \text{ °C}$ (for approx. 48 h) to optical density of at least 1.4 at 660 nm [24] on a Jenway 6305 UV/Visible Spectrophotometer (Bibby Scientific, UK). Hereafter, the yeast cells were washed 3 times with fresh YEPD. After the final wash, the yeasts were resuspended in YEPD medium containing 20% glycerol serving as a cryo-protector [25]. These suspensions were aliquoted into different portions and vortexed to ensure homogeneous distribution of the yeast cells. Subsequently, these samples were frozen at -80 °C until needed. Strain DLY640 represented WT with an optimum growth temperature of $\sim 35 \text{ °C}$ [15,16], and DLY1108 strain (*cdc13-1* temperature sensitive mutant) possessed a point mutation in CDC13 gene. The optimum growth temperature of the mutant is between 22 and 24 °C.

2.3. HTM measurements

The growth of yeast based on the analysis of heat-flow through electrode surfaces was evaluated using a home-made device, whose design was previously described in ref 4. Type K thermocouples (Onecall, Leeds, UK) were inserted into flow cells that were coupled to the HTM equipment and used to measure the temperature at the heat sink and in the solution. The temperature at the heat sink (T_1) was actively controlled with a Proportional-Integral-Derivative (PID) controller. The second thermocouple was placed in the liquid at 1.7 mm above the electrode surface to monitor the temperature of the solution.

The heat-transfer resistance (R_{th}) between the thermocouples was then obtained by dividing the temperature gradient over the power required to keep T_1 at the set temperature (see ref [4–6] – and Equation (1)). Initially, measurements were performed in a standard Perspex flow cell that has been well described in literature [4]. However, the design had to be revisited due to the build-up of gasses in the flow cell, which led to significant interference with the R_{th} signal. Therefore, a novel design was constructed in Solid Works (2016, 3D CAD SP4) and 3D-printed with in-house facilities. This design is schematically shown in Fig. 1.

R_{th} calculation

$$R_{th} = \frac{(T_1 - T_2)}{P} \quad (1)$$

These models were printed with a FORM2 stereolithography printer from Formlabs (USA) with a layer height of 25 μm . FORM2 Clear Resin (GPCL04) was used as resin and uncured polymer resin was removed by washing with isopropanol [19]. The printed flow cell was then fully cured in a UV post-print chamber, which will guarantee complete polymerization. The screw holes were provided with M3 tapping to allow secure attachment of the copper lid. These flow cells were used in all HTM measurements where the growth of yeast was evaluated. Prior to analysis and mounting of the samples into the flow cell, the electrodes were cleaned by washing with ammonia and piranha solution (RCA standard cleaning procedure ref 27).

Optimization of the PID settings to minimize the noise on the signal was performed on all three electrodes prior to their evaluation on the relation between yeast concentrations and thermal resistance. Initially, electrodes were stabilized into a solution of YEPD medium after which solutions of yeast with increasing CFU/mL (10^2 – 10^7 CFU/mL) were added. This was done stepwise at 1 h intervals where each cell suspension (increasing concentration) was injected with a flowrate of 200 $\mu\text{L}/\text{min}$ using a NE-500 Syringe pump (ProSense, the Netherlands).

To study the microorganism growth, a yeast culture of known concentration was injected into the. Subsequently, an influx of fresh YEPD medium was initiated at a flowrate of 800 $\mu\text{L}/\text{h}$, which ensured sufficient exchange of nutrients and removal of build-up gasses. The thermal resistance was monitored over time, with T_1 kept constant at 37 °C for

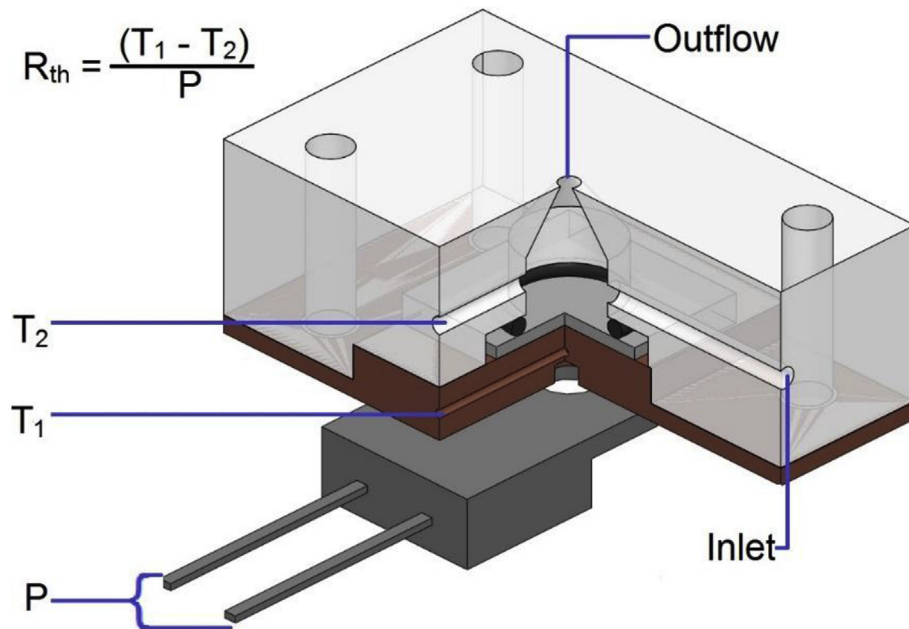


Fig. 1. Schematic lay-out of the 3D printed flow cell where the outlet is moved to the top to facilitate gas removal. The thermal resistance is determined by dividing the temperature gradient ($T_1 - T_2$) by the power (P) required to keep the heat sink at a fixed temperature.

Table 1

Optimized PID settings for a range of electrodes when thermal resistance was measured for 60 min at $37 \pm 0.02^\circ\text{C}$ in PBS.

Electrode	Thermal Conductivity (W/K m)	P	I	D	R_{th} ($^\circ\text{C}/\text{W}$)	StDev ($^\circ\text{C}/\text{W}$)	Percentage error (%)
Au	318 [31]	1	11	0	2.46	0.02	0.85
Au/Pd	59 [30]	1	9	0.2	3.69	0.04	0.96
Si	149 [31]	1	9	0.1	3.57	0.03	0.75

all experiments involving the WT strain and at 25°C for the mutant, except for the evaluation the growth rate. For the latter, the temperature was increased every 5 h by 1°C , with a starting temperature of 19°C .

2.4. Validation of thermal results with agar plating methods

The influence of the nutrient composition, temperature and addition of toxic copper on the growth of yeast cells was studied. This was done by comparing the evolution of thermal resistance in nutrient rich medium over time to that of nutrient poor medium (ex-YEPD), to yeast that was exposed to 95°C for 10 min, and in the presence of copper sulfate ($0.15\text{ mM Cu}_2\text{SO}_4$ in YEPD). These thermal measurements were validated using plating techniques, for which conventional agar YEPD plates were used for scoring viability at values ranging between 10^2 and 10^5 CFU/mL . These plates were inoculated with $100\text{ }\mu\text{L}$ of cell suspensions at certain dilutions and incubated for at least 24 h at a selected optimal growth temperature. These experiments were performed in YEPD and under growth inhibiting conditions, including the use of ex-YEPD, yeast exposed to heat shocks and the addition of copper to either the plates or the medium. At higher CFU/mL values, optical density was used to validate results.

3. Results and discussion

3.1. PID optimization of electrodes and studying different concentrations of yeast cells

Previous work by Geerets et al. [29], demonstrated that the optimization of the PID parameters of the HTM set up is the key to minimizing noise on the signal and has a significant impact on the limit of detection. In addition, it was necessary to investigate whether yeast adheres to electrodes since this is required in order to monitor changes in the heat-transfer resistance.

A gold-coated silicon electrode, electrode consisting of a mixture of gold and palladium (80% Au and 20% Pd), or a silicon electrode was mounted into the flow-cell. Hereafter, the flow chamber was filled up with PBS and the system was allowed to stabilize to its pre-set temperature over the next 1 h. The thermal conductivity for each electrode material are obtained from literature and reported in Table 1 [30,31]. To compensate for the difference in the thermal conductivity between each of the electrodes, the PID feedback loop will need to be optimized.

The proportional component (P) depends on the difference between the set point and process variable. Increasing P will lead to increasing the speed of control in the reaction but if it is too high, oscillations will occur in the system. Therefore, there needs to be a trade-off in the resistance of the system to temperature fluctuations and the noise in the signal. The integral component (I) sums the error over time and is used to drive the error over time to zero. The derivative term (D) is used to predict errors in the future and is not varied much since high values lead to large instabilities in the system. The optimum PID settings will have the lowest standard deviation on the signal, and hence will enhance the sensitivity of the developed sensors.

It can be observed that the electrodes exhibit different R_{th} values, which is due to differences in thickness and conductivity of the materials. Gold is the best conductor and was therefore expected to have the lowest thermal resistance, as was observed. The standard deviation, determined as the average of 600 points, was divided over the absolute value of the thermal resistance and multiplied by 100 to obtain the percentage error. It can be seen in Table 1 that these values for all electrodes fell in the same range, and are similar to that previously reported in the literature [4–6].

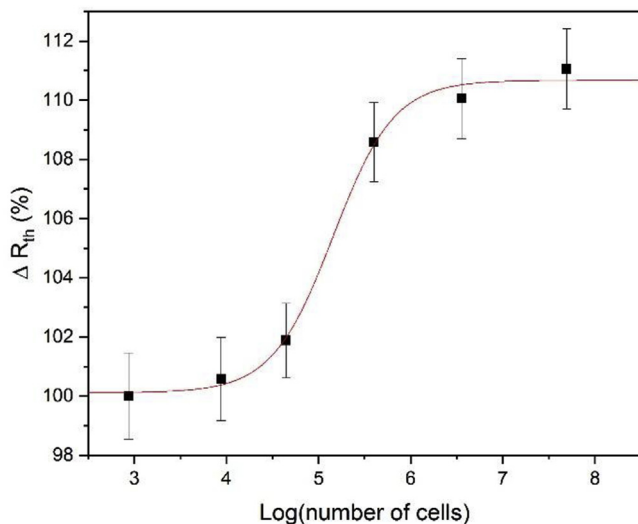


Fig. 2. The difference in thermal resistance when gold-coated electrodes that were exposed to different concentrations of yeast cells in YEPD medium ($T_1 = 37^\circ\text{C}$). The curve was fitted with a standard dose-response fit ($R^2 = 0.99$). Standard deviations were determined by taking the average of at least 600 points. (For interpretation of the references to colour in this figure legend, the reader is referred to the Web version of this article.)

First, the thermal response of these electrodes to PBS buffer with a number of increasing concentrations of yeast cells was studied. As can be seen in [Figure S-1](#), all electrodes exhibited higher R_{th} values with increasing amount of cells. However, the gold-coated electrodes proved to be the most sensitive and had the widest dynamic range (10^4 – 10^7 CFU/mL). Therefore, a study with a wider range of yeast concentrations in YEPD (10^3 – 10^8 CFU/mL) was performed with this type of electrodes, which served as a calibration for the system ([Fig. 2](#)).

[Fig. 2](#) demonstrates that the measured thermal resistance depends on the amount of yeast cells. The linear range was from 10^4 – 10^7 CFU/mL, after which saturation of the electrodes occurred with yeast. Vigorous rinsing (syringe pump at highest rate) was performed between the additions to minimize adhesion of cells to the surface. Prior to the HTM measurements the CFU/mL values were obtained with standard UV-vis (10^6 – 10^8 CFU/mL), this was not possible for lower concentrations, where values were obtained by cell counting after plating of the yeast (10^3 – 10^5 CFU/mL). At values ranging from 10^5 to 10^6 CFU/mL plating and spectrophotometrically determination were not able to accurately determine the number of yeast cells, explaining why no measurement data are provided in this region.

These measurements were performed with the flow cell design described in Refs. [3,4]. However, spikes in the thermal resistance were observed after several hours, which was due to the formation of gas (CO_2) that builds up during yeast growth. While this allows the number of yeast cells to be estimated, the set up could not be employed for the studying of yeast growth over time. Adjustments to the set-up, such as incorporation of a gas membrane or increasing the flow rate of the medium, were either not successful or led to significant disturbances in the thermal signal. Therefore, all further experiments were performed with a revised flow cell design shown in [Fig. 2](#).

3.2. Evaluation of yeast growth under different conditions employing 3D fabricated flow cells

To determine whether this novel design that features an outlet at the top of the flow cell was capable of measuring yeast growth rates, blank measurements were performed. Therefore, solutions of YEPD were measured over 14 h at temperatures of 30 and 37°C in the absence of yeast cells ([Fig. 3](#)).

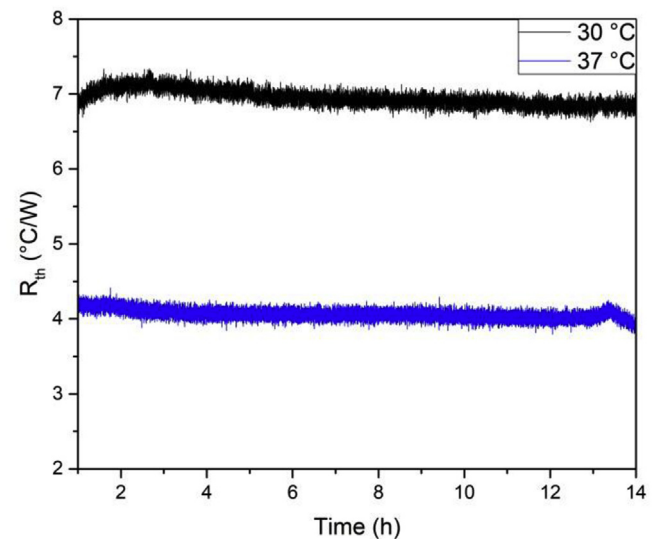


Fig. 3. The temperature dependent thermal resistance. T_1 is set to either 30 or 37°C and the R_{th} is monitored for over time while a flow rate of 800 $\mu\text{L/h}$ was applied exchanging the YEPD over the gold electrode. (For interpretation of the references to colour in this figure legend, the reader is referred to the Web version of this article.)

When gold electrodes were measured at 30°C , the signal stabilized at $6.95 \pm 0.1^\circ\text{C/W}$ after 1 h. This value is lower than when measurements were performed at 37°C ($4.06 \pm 0.06^\circ\text{C/W}$) due higher deception of heat to the environment. After 14 h, for both measurements no significant difference was observed which confirms the establishment of appropriate baselines. This thermal resistance deviates from measurements performed in the previous flow cell due to differences in distribution of thermal flow across the flow cell. Measurements were performed in triplicate, with similar starting values (standard deviation 0.1°C/W).

Subsequently, these references were compared to when yeast cells (WT) were present under conditions optimized for the highest replication rate of the yeast cells (800 $\mu\text{L/h}$ of fresh YEPD, $T = 37^\circ\text{C}$). The starting concentration of yeast in YEPD was equal to approximately 10^4 CFU/mL and the thermal resistance was monitored over 60 h. The same growth experiment was conducted with the DLY1108 strain at its optimal growth temperature, which is $\sim 23^\circ\text{C}$. [Fig. 4](#) shows the thermal resistance over time for both yeast strains, with an average of the thermal resistance taken every hour. Standard deviation was determined by averaging out at least 3600 data points.

The difference in initial thermal resistance ($3.5 \pm 0.1^\circ\text{C/W}$ for WT and $5.9 \pm 0.1^\circ\text{C/W}$ for the mutant strain, respectively) is due to the fact that the measurements were conducted at different temperatures. However, a clear increase in thermal resistance was observed for both strains with a 15% increase for the WT and a 9% increase for the DLY1108 mutant strain over 42 h. A lower increase was expected for the mutant strain since the mutation diminishes the growth rate.

For the WT yeasts, the thermal resistance changes at a rate of $\sim 0.06^\circ\text{C/W}$ per hour until 20 h, after which saturation of the signal was observed. This is due to full coverage of the electrode, meaning that further replication will push the yeast cells away from the surface into the solution decreasing the effect on the change in thermal resistance to approximately 0.02°C/W per hour. Measurements were performed in triplicate, with growth rates ranging from 0.04 to 0.06°C/W per hour for the first 20 h. It has to be noted this depends on the initial concentration of yeast cells and the temperature at which the experiment is conducted.

The lower the temperature, the more prone the signal is to perturbations in the external temperature, to minimize this effect the flow cells were placed in an incubator. However, minor fluctuations were

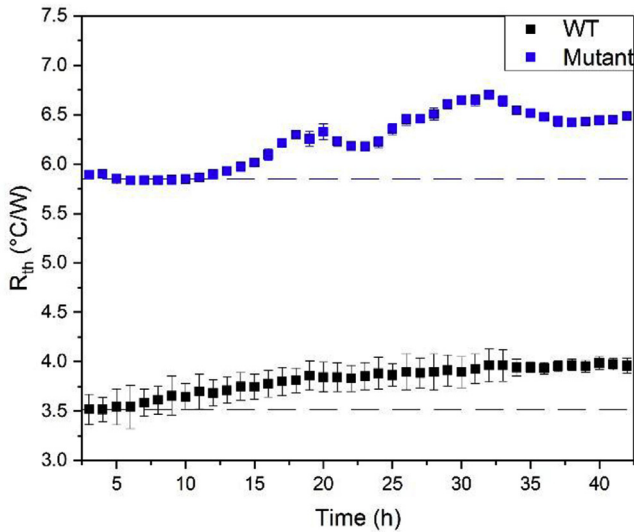


Fig. 4. The hourly average R_{th} value of a standard growth curve for both the WT and mutant strain. Both measurements were started with $\sim 10^4$ CFU/mL where the WT strain (black) was grown at 37 °C and the DLY1108 mutant (blue) at 25 °C. The graph is displayed starting 0.5 h after the injection of the yeasts thereby accounting for the initial stabilisations. The error bars indicating the standard deviation over 3600 points. (For interpretation of the references to colour in this figure legend, the reader is referred to the Web version of this article.)

observed on strain mutant stain (around 30 h), leading to an overall rate of change in thermal resistance of 0.02 °C/W per hour. The replication rate of this mutant strain is lower compared to the WT, hence, saturation of the surface is not occurring yet.

Subsequently, it was evaluated whether kinetic effects could be studied by comparing the growth of the WT (optimal growth ~ 37 °C) and mutant yeast strain (optimal growth ~ 23 °C) at various temperatures. The mutation in the *CDC13* gene leads to cell cycle arrest at temperature above 30 °C, meaning the cells remain viable for a certain amount of time but do not replicate. These experiments were performed to quantify yeast growth, and evaluate to what extent growth is affected by external parameters.

Flow cells were placed in an incubator set to 25.0 °C for all WT yeast and to 15.0 °C for experiments with the mutant strain, ensuring minimal disruption to the signal by external effects, such as temperature fluctuations. For the mutant strain, the temperature of the heat sink was varied from 17 °C to 31 °C in steps of 1 °C every 5 h. Yeast cells were injected with a starting value of $\sim 10^4$ CFU/mL.

The thermal resistance is highly dependent on the temperature gradient ($T_1 - T_2$). This gradient is larger at lower temperatures, explaining the decreases in R_{th} that were observed by increasing the temperature. Table 2 shows that there are differences in the increases in thermal resistance at various temperatures. The growth kinetics for each yeast strain were determined according to Equation (2) where initial stabilization time (t_{stab}) (30 min) is subtracted from the measurement time (t_{meas}) (5 h).

Determination of growth rate

$$\text{Growth rate} = \frac{\Delta R_{th}}{(t_{meas} - t_{stab})} \quad (2)$$

The temperature (T_1) was varied in the range between 30 °C and 51 °C for WT yeasts and between 17 °C and 35 °C for the mutant strain with steps of 1 °C every 5 h. A minimal number of 16200 points was used to increase accuracy of the results. Table 2 shows that the highest growth rate at a temperature of 38 °C for WT (0.143 °C/W per h) and at 24 °C for the mutant strain (0.051 °C/W per h). The growth rates at the remaining temperatures were normalised to these values, respectively.

Table 2

Growth kinetics of the WT (T ranging 30–50 °C) and the mutant strain (T ranging from 21 to 33 °C). Values were normalised and compared to the highest growth rate.

WT strain				Mutated strain			
T_1	T_2	Growth rate	Normalised signal	T_1	T_2	Growth rate	Normalised signal
°C	°C	°C/W per h	%	°C	°C	°C/W per h	%
30	29.30	0.016	11	21	19.27	0.049	96
31	29.99	0.033	23	22	20.94	0.020	39
32	30.96	0.030	21	23	21.01	0.026	50
33	31.75	0.041	29	24	22.14	0.051	100
34	32.88	0.010	7	25	23.45	0.027	52
35	33.60	0.035	24	26	23.97	0.051	99
38	35.56	0.143	100	27	24.84	0.016	31
39	36.27	0.060	42	28	25.74	0.028	55
40	37.78	0.050	35	29	26.68	0.029	58
42	40.33	0.045	31	30	27.62	0.022	43
45	42.94	0.013	9	31	28.63	0.017	34
50	42.98	0.065	45	32	29.48	0.016	31
51	43.96	0.054	38	33	30.32	0.023	46

For each 5 h (30 min initial stabilization) incubation period the slope of the signal was determined using a standard linear fit.

Table 2 shows that, below 40 °C, there is approximately 1 °C difference between the temperature of the heat sink (T_1) and the temperature of the fluid (T_2) at 1.7 mm above the chip surface. The temperature of the yeast on the electrode will therefore be between those values. It is also observed that the WT strain replicates $20 \pm 5\%$ faster than the mutant strain, which is in accordance with the data shown in Fig. 5. For the WT, the data in Table 2 were used to construct a Gaussian distribution of the growth rate (Fig. 6). This shows that the WT strain replicates fastest at 37 °C, which is in accordance with what is described in literature [16].

3.3. Inhibition of yeast growth by controlling temperature, medium, and addition of toxic compounds to the flow cell

Subsequently, the impact of different parameters (temperature, medium and toxic compounds) on the growth of the WT yeast strain was evaluated. First, yeast ($\sim 10^5$ CFU/mL) was added to the flow cell

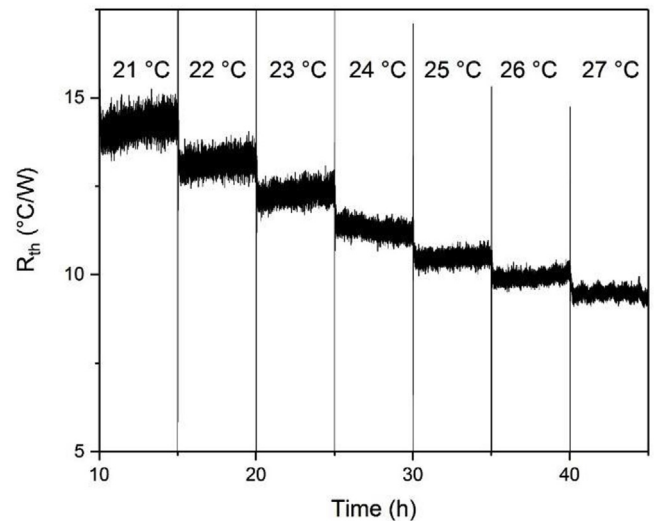


Fig. 5. Growth behaviour of the mutant strain (starting concentration $\sim 10^4$ CFU/mL), where temperature of the copper heat sink was varied in steps of 1 °C every 5 h. A constant flow rate of 800 μ L/h of a fresh YEPD solution was applied to ensure yeast was kept under optimal growth conditions.

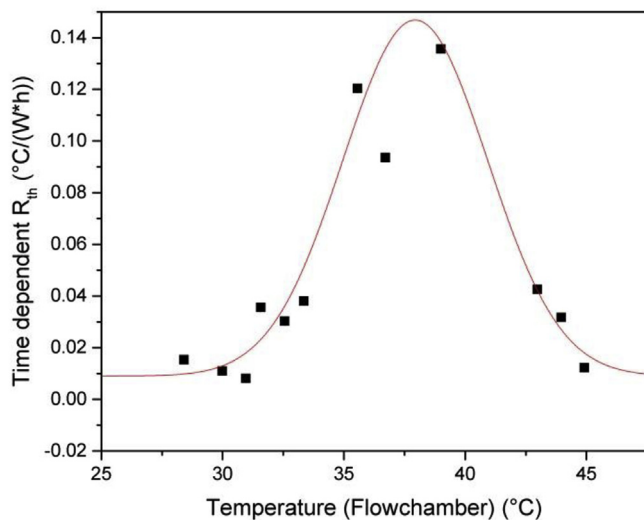


Fig. 6. Time dependent R_{th} values ($^{\circ}\text{C}/\text{W}$ per h) for growth of WT. Values are shown for T_2 values ranging between 27°C and 45°C . Line represents a Gaussian fit ($R^2 = 0.99$).

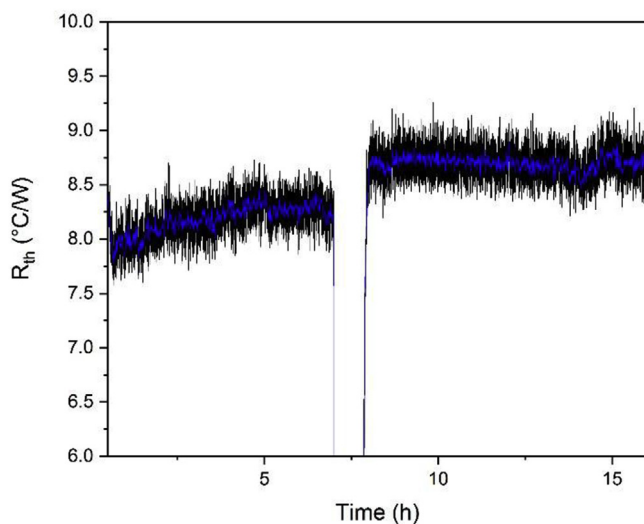


Fig. 7. Thermal elimination (at 99°C) of WT yeast. The measurement was started with $\sim 10^5$ CFU/mL of WT yeast that were grown at 37°C for 7 h. Hereafter, the temperature of T_1 was increased (in 10 min) to and kept at 99°C for 10 min before returning back to 37°C (in 20 min). This thermally eliminated the yeast culture as is clearly demonstrated with elevated R_{th} value (due to disintegration of the cells) that remains constant. The blue line is a gentle median filter (50 points) applied to the raw data (black line). (For interpretation of the references to colour in this figure legend, the reader is referred to the Web version of this article.)

at $T_1 = 37^{\circ}\text{C}$ and an increase in thermal resistance was observed. After 7 h, the temperature was increased to 99°C for 15 min to eliminate the yeast cells. Hereafter, the temperature was decreased to 37°C where no additional increase was observed, as is shown in Fig. 7.

When yeast was replicating at 37°C , the R_{th} signal increased with $0.06^{\circ}\text{C}/\text{W}$ per h, which is similar to that stated in Table 2. After boiling the yeast, the thermal resistance increased by $0.5 \pm 0.1^{\circ}\text{C}/\text{W}$, but remained stable over time. The increase in signal can be attributed to the disintegration of dead yeast cells that sink to the bottom, thereby creating a dense layer on the electrode that blocks heat-flow through the surface. This has been confirmed with data in Supporting Information Figure S-3, which shows that we are able to determine concentrations of dead yeast cells but no increase of the thermal

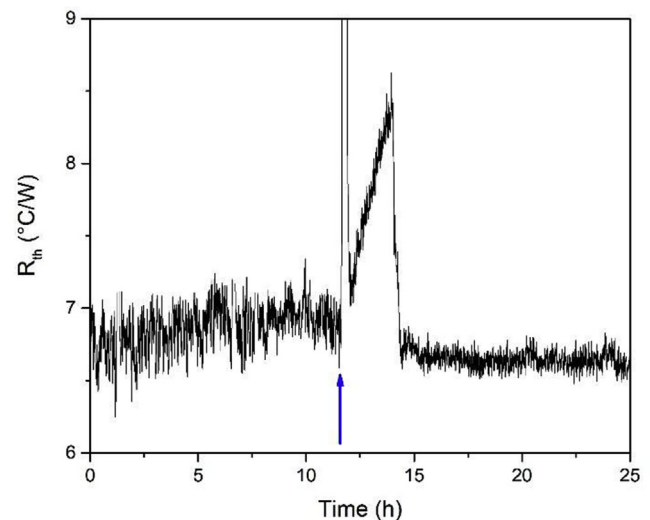


Fig. 8. The influence of copper sulphate on the growth of WT yeast cells. Normal growth of WT yeast in YEPD at 37°C shows an increase in thermal resistance, blue line is when medium was exchanged to medium containing 15 mM Cu_2SO_4 . (For interpretation of the references to colour in this figure legend, the reader is referred to the Web version of this article.)

resistance over time (hence, no replication) was observed. The flow rate of $800 \mu\text{L}/\text{h}$ used in this experiment was not sufficient to remove the dead yeast from the surface and higher flow rates would have disturbed the experiment.

Plating techniques confirmed that yeast was growing at a normal rate at 37°C and no growth was observed when the yeast was incubated at 99°C for 10 min.

Second, the growth of yeast was evaluated when it was exposed to copper ions. To this end, a solution of 15 mM Cu_2SO_4 in YEPD was used and the yeast was incubated in the solution for 2 h (indicated by the blue arrow). The results are shown in Fig. 8.

At the time indicated by the blue arrow, the medium was exchanged to 15 mM Cu_2SO_4 and left to incubate for 2 h (no flow during the incubation). Hereafter, the medium was gradually exchanged back to YEPD at a flow rate of $800 \mu\text{L}/\text{h}$. This means continuously cold medium is pumped into the flow cell, which means the power has to be increased in order to bring the fluid in the flow cell back to 37°C . However, after the exchange of the medium the signal returns back to the baseline level. Fig. 8 clearly demonstrates that no yeast growth is observed after addition of copper ions to the solution. This was confirmed by measurements with plating experiments (Figure S-2).

Finally, the influence of the medium was evaluated. The growth kinetics were compared between yeast in YEPD and in ex-YEPD, which lacks nutrients for the microorganism to be able to grow. Initially, yeast growth of $0.06^{\circ}\text{C}/\text{W}$ per hour was observed, corresponding to Table 2. After exchanging the medium to ex-YEPD at 24 h, no significant increases in thermal resistance were reported. These results are shown in Fig. 9.

Fig. 9 clearly demonstrates the differences in yeast growth rate when comparing YEPD medium to ex-YEPD. However, if the cells lack nutrients they first entered an arrested cell state and can survive for several hours. In Supporting Information S-4, it is shown that this is a reversible process. After 14 h of incubation in ex-YEPD, the medium was gradually exchanged to YEPD and this restored the growth properties of the yeast. However, it has to be noted that the increase in thermal resistance is not as pronounced as before the incubation in ex-YEPD, this could indicate that the optimum conditions are not fully restored for all yeast cells in this short incubation time.

This work uses *S. cerevisiae* as a model organism to demonstrate that growth behaviour of microorganisms can be studied in real-time with

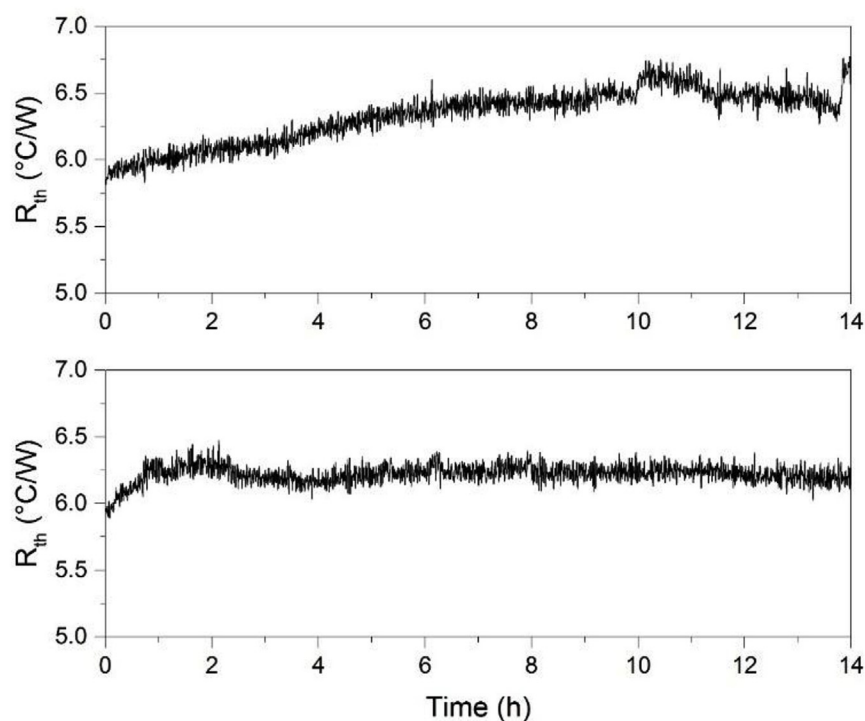


Fig. 9. The influence of the medium on the growth of WT cells at 37 °C. The top graph shows the first 14 h of the measurement during which the cells are able to grow providing a constant flow (800 µL/h) of fresh YEPD broth. The bottom graph shows the same culture after the medium has been fully exchanged using a constant 800 µL/h flow rate of ex-YEPD.

thermal detection methods. In the future, the idea is to expand this to other microorganism such as bacteria and fungi. This means we could study the influence of drug compounds (such as antibiotics) on bacterial growth, which would help to determine the appropriate course of treatment for bacterial infections. It can also be used to evaluate the efficacy of antimicrobial coatings since this technique is sensitive to the concentration of bacteria at the interface. Furthermore, since it enables *in real-time* measurements, it can be employed to monitor microorganism levels on-site in for instance in water pipes or water supplies in hospitals, indicating when contamination occurs or when cleaning is required.

4. Conclusions

In this work, we used *S. cerevisiae* as a model organism to demonstrate that the growth behaviour of microorganisms can be analysed using the Heat-Transfer Method (HTM). It was experimentally determined that higher concentrations of *S. cerevisiae* (WT) cells in buffered solutions cause a higher thermal resistance at the interface between the electrode and liquid. Different electrodes (Au, Au/Pd and Si) were evaluated for their performance and thermal response in buffered solution. Gold electrodes were used in all further experiments because of their excellent stability, minimal noise on the signal (0.83% at 37 °C) and wide dynamic range (10^3 – 10^7 CFU/mL), allowing for the accurate quantification of *S. cerevisiae* cultures.

In order to measure growth of *S. cerevisiae* the flow cell was redesigned by incorporating a gas outlet. These flow cells where 3D-printed with FORM2 Clear Resin, enabling easy scale up of production thereby increasing the commercial potential of the method. These new flow cells showed a clear increase in thermal resistance over time when either WT or mutant strains where measured under optimal conditions, indicating the growth of *S. cerevisiae*.

The concentrations measured by thermal analysis were confirmed by standard plating methods and UV determination, depending on the final concentration of the yeast.

In addition, reference measurements with dead yeast (caused by incubation at 99 °C for 10 min prior to measurement) and yeast in medium depleted of nutrients did not show differences in the thermal

resistance over time. Inhibition of growth was observed by exposing yeast to either elevated temperatures or addition of copper solutions to the flow cell. Finally, thermal analysis was used to study growth kinetics of WT and a mutant strain by monitoring the increase in thermal resistance after applying certain temperature ramps. The highest growth rate found using thermal analysis is in agreement with what has been reported in literature [28]. The temperature corresponding with this gradient of the thermal resistance can be used to quantify replication, allowing a direct comparison on the external parameters influencing microbial growth.

This is the first report of the use of HTM for *in real-time* analysis of microorganism growth. The advantage of this thermal sensing is its simplicity, low-cost and use of a portable set up that does not require a lab environment. The methodology described is versatile and can be extended to evaluate other microorganisms, which has great potential for evaluating the response of bacteria to selected (antibiotic) drug compounds.

Acknowledgements

We would like to acknowledge the Advanced Materials and Surface Engineering Centre at Manchester Metropolitan University for funding the PhD of KB. Furthermore, we would like to thank the Royal Society of Chemistry for support with consumables (Research Fund RF182-811 of MP) and enabling international collaborations (Researcher Mobility grant of MP).

Appendix A. Supplementary data

Supplementary data related to this article can be found at <http://dx.doi.org/10.1016/j.phmed.2018.05.001>.

References

- [1] J. Wang, Electrochemical biosensors: towards point-of-care cancer diagnostics, *Biosens. Bioelectron.* 21 (2006) 1887–1892.
- [2] M.A. Cooper, Label-free screening of bio-molecular interactions, *Anal. Bioanal. Chem.* 377 (2003) 834–842.
- [3] B. van Grinsven, K. Eersels, M. Peeters, P. Losada-Pérez, T. Vandenryt, T.J. Cleij,

- P. Wagner, The heat-transfer method: a versatile low-cost, label-free, fast, and user-friendly read out platform for biosensor applications, *ACS Appl. Mater. Interfaces* 6 (2014) 11309–11318.
- [4] B. van Grinsven, N. Vanden Bon, H. Strauven, L. Grieten, M. Murib, K.L. Jiménez-Monroy, S.D. Janssens, K. Haenen, M.J. Schöning, V. Vermeeren, M. Ameloot, L. Michiels, R. Thoen, W. de Ceuninck, P. Wagner, Heat-transfer resistance at solid-liquid interfaces: a tool for the detection of single-nucleotide polymorphisms in DNA, *ACS Nano* 6 (2012) 2712–2721.
 - [5] K. Eersels, B. van Grinsven, A. Ethirajan, S. Timmermans, K. Jiménez-Monroy, J.F. Bogie, S. Punniyakoti, T. Vandenryt, J.A. Hendriks, T.J. Cleij, M.J.A.P. Daemen, V. Somers, W. De Ceuninck, P. Wagner, Selective identification of macrophages and cancer cells based on thermal transport through surface-imprinted polymer layers, *ACS Appl. Mater. Interfaces* 5 (2013) 7258–7267.
 - [6] F. Canfarotta, J. Czulak, K. Betlem, A. Sachdeva, K. Eersels, B. van Grinsven, T.J. Cleij, M. Peeters, A novel thermal detection method based on molecularly imprinted nanoparticles as recognition elements, *Nanoscale* 10 (2018) 2081–2089.
 - [7] P. Losada-Pérez, K.L. Jiménez-Monroy, B. van Grinsven, J. Leys, S.D. Janssens, M. Peeters, C. Glorieux, J. Thoen, K. Haenen, W. De Ceuninck, P. Wagner, Phase transitions in lipid vesicles detected by a complementary set of methods heat-transfer measurements, adiabatic scanning calorimetry and dissipation-mode quartz crystal microbalance, *Phys. Status Solidi* 211 (2014) 1377–1388.
 - [8] D. Botstein, S.A. Chervitz, J.M. Cherry, Yeast as a model organism, *Science* 277 (5330) (1997) 1259–1260.
 - [9] H. Karathia, E. Vilapriyo, A. Sorribas, R. Alves, *Saccharomyces cerevisiae* as a model organism: a comparative study, *PLoS One* 6 (2011) e16015.
 - [10] R. Li, A.W. Murray, Feedback control of mitosis in budding yeast, *Cell* 66 (1991) 519–531.
 - [11] W.-K. Huh, J.V. Falvo, L.C. Gerke, A.S. Carroll, R.W. Howson, J.S. Weissman, E.K. O'Shea, Global analysis of protein localization in budding yeast, *Nature* 425 (2003) 686–691.
 - [12] I. Herskowitz, Life cycle of the budding yeast *Saccharomyces cerevisiae*, *Microbiol. Rev.* 52 (1988) 536–544.
 - [13] C. Rosa, G. Péter, *Biodiversity and Ecophysiology of Yeasts*, Springer, Berlin, 2006.
 - [14] Wood, L. Hartwell, A dependent pathway of gene functions leading to chromosome segregation in *Saccharomyces cerevisiae*, *J. Cell Biol.* 94 (1982) 718–726.
 - [15] M. Zubko, D. Lydall, Linear chromosome maintenance in the absence of essential telomere-capping proteins, *Nat. Cell Biol.* 8 (2006) 734–740.
 - [16] M.K. Zubko, S. Guillard, D. Lydall, EXO1 and RAD24 differentially regulate generation of ssDNA at telomeres of *Saccharomyces cerevisiae* cdc13-3 mutants, *Genetics* 168 (2004) 103–115.
 - [17] Z. Salvadó, F.N. Arroyo-López, J.M. Guillamón, G. Salazar, A. Querol, E. Barrio, Temperature adaptation markedly determines evolution within the genus *Saccharomyces*, *Appl. Environ. Microbiol.* 77 (2011) 2292–2302.
 - [18] T. Münch, B. Sonnleiter, A. Fiechter, New insights into the synchronization mechanism with forced synchronous cultures of *Saccharomyces cerevisiae*, *J. Biotechnol.* 24 (1992) 299–314.
 - [19] C. Beck, H. Kaspar von Meyenburg, Enzyme pattern and aerobic growth of *Saccharomyces cerevisiae* under various degrees of glucose limitation, *J. Bacteriol.* 96 (1968) 479–486.
 - [20] W. Woodside, H. Messmer, Thermal conductivity of porous media, *J. Appl. Phys.* 32 (1961) 1688–1699.
 - [21] K. Betlem, M.P. Down, C.W. Foster, S. Akthar, K. Eersels, B. van Grinsven, T.J. Cleij, C.E. Banks, M. Peeters, Development of a flexible MIP-based biosensor platform for the thermal detection of neurotransmitters, *MRS Advances* (2018) 1–6.
 - [22] R. Festa, D. Thiele, Copper at the front line of the host-pathogen battle, *PLoS Pathog.* 8 (2012) e1002887.
 - [23] C. Molteni, H.K. Abicht, M. Solioz, Killing of bacteria by copper surfaces involves dissolved copper, *Appl. Environ. Microbiol.* 76 (2010) 4099–4101.
 - [24] D. Yasokawa, S. Murata, E. Kitagawa, Y. Iwahashi, R. Nakagawa, T. Hashido, H. Iwahashi, Mechanisms of copper toxicity in *Saccharomyces cerevisiae* determined by microarray analysis, *Environ. Toxicol.* 23 (2008) 599–606.
 - [25] D. Burke, D. Dawson, T. Stearns, *Methods in Yeast Genetics*, Cold Spring Harbor Laboratory, New York, 2000, p. 144.
 - [26] M. Peeters, B. van Grinsven, T.J. Cleij, K.L. Jiménez-Monroy, P. Cornelis, E. Pérez-Ruiz, G. Wackers, R. Thoen, W. De Ceuninck, J. Lammertyn, P. Wagner, Label-free protein detection based on the heat-transfer method: a case study with the peanut allergen Ara h1 and aptamer-based synthetic receptors, *ACS Adv. Mater. Interfaces* 7 (2015) 16–23.
 - [27] C. Kurtzman, J. Fell, *The Yeasts: a Taxonomic Study*, Elsevier, Amsterdam, 2011.
 - [28] S. Wolf, R. Tauber, *Silicon Processing for the VLSI Era Volume 1: Process Technology*, Lattice Press, Sunset Beach, Calif, 1986, pp. 516–517.
 - [29] B. Geerets, M. Peeters, B. Grinsven, K. Bers, W. de Ceuninck, P. Wagner, Optimizing the thermal read-out technique for MIP-based biomimetic sensors: towards nanomolar detection limits, *Sensors* 13 (2013) 9148–9159.
 - [30] R.L. Powell, W.A. Blanpied, *Thermal Conductivity Of Metals And Alloys At Low Temperatures: A Review Of The Literature*, ADA279118, National Bureau of Standards Gaithersburg MD, 1954.
 - [31] J.A. Dean, N.A. Lange, *Lange's Handbook of Chemistry*, McGraw-Hill, 1999 section 4.1.